

## Structure - Function Relationships in the Stem Cell's Mechanical World B: Emergent Anisotropy of the Cytoskeleton Correlates to Volume and Shape Changing Stress Exposure

Hana Chang\* and Melissa L. Knothe Tate\*,†,‡

**Abstract:** In the preceding study (Part A), we showed that prescribed seeding conditions as well as seeding density can be used to subject multipotent stem cells (MSCs) to volume changing stresses and that changes in volume of the cell are associated with changes in shape, but not volume, of the cell nucleus. In the current study, we aim to control the mechanical milieu of live cells using these prescribed seeding conditions concomitant to delivery of shape changing stresses via fluid flow, while observing adaptation of the cytoskeleton, a major cellular transducer that modulates cell shape, stiffness and remodeling. We hypothesize that the spatiotemporal organization of tubulin and actin elements of the cytoskeleton changes in response to volume and shape changing stresses emulating those during development, prior to the first beating of the heart or twitching of muscle. Our approach was to quantify the change over baseline in spatiotemporal distribution of actin and tubulin in live C3H/10T1/2 model stem cells subjected to volume changing stresses induced by seeding at density as well as low magnitude, short duration, shape changing (shear) stresses induced by fluid flow (0.5 or 1.0 dyne/cm<sup>2</sup> for 30/60/90 minutes). Upon exposure to fluid flow, both tubulin thickness (height) and concentration (fluorescence intensity) change significantly over baseline, as a function of proximity to neighboring cells (density) and the substrate (apical-basal height). Given our recently published studies showing amplification of stress gradients (flow velocity) with increasing distance to nearest neighbors and the substrate, *i.e.* with decreasing density and toward the apical side of the cell, tubulin adaptation appears to depend significantly on the magnitude of the stress to which the cell is exposed locally. In contrast, adaptation of actin to the changing mechanical

---

\* Department of Biomedical Engineering, Case Western Reserve University, 2071 Martin Luther King Jr. Drive, Cleveland, OH 44106-7207

† Department of Mechanical & Aerospace Engineering, Case Western Reserve University, 2123 Martin Luther King Jr. Drive, Cleveland, OH 44106-7207

‡ Corresponding author. Phone: (216)-368-5884; Fax: (216)-368-4969; knothenate@case.edu

milieu is more global, exhibiting less significant differences attributable to nearest neighbors or boundaries than differences attributable to magnitude of the stress to which the cell is exposed globally (0.5 versus 1.0 dyne/cm<sup>2</sup>). Furthermore, changes in the actin cytoskeletal distribution correlate positively with one pre-mesenchymal condensation marker (*Msx2*) and negatively with early markers of chondrogenesis (*Col11a1* alone, indicative of pre-hypertrophic chondrogenesis) and osteogenesis (*Runx2*). Changes in the tubulin cytoskeletal distribution correlate positively with a marker of pericondensation (*Sox9* alone), negatively with chondrogenesis (*Col11a1*) and positively with adipogenesis (*Ppar-γ2*). Taken as a whole, exposure of MSCs to volume and shape changing stresses results in emergent anisotropy of cytoskeletal architecture (structure), which relate to emergent cell fate (function).

**Keywords:** developmental biology, mechanobiology, wound healing, tissue engineering, regenerative medicine, stem cell, cytoskeleton, mechanical adaptation, shear stress, anisotropy, cell and nucleus shape, seeding density, tubulin, actin

## 1 Introduction

Cell shape and fate (lineage commitment) are intrinsic manifestations of form and function at the cellular and subcellular scales [3], and stem cells exhibit up to a 1000-fold greater capacity to sense and adapt to their local mechanical environment than differentiated cells of musculoskeletal lineages [3-7]. An understanding of stem cell mechanoadaptation is key to deciphering how stem cells commit to a particular fate or lineage (differentiate), both during prenatal development, wound healing and regeneration, as well as *de novo* engineering of tissues. Our working hypothesis is that the mechanical structure of stem cells emerges from their local mechanical milieu. Over time, persistence of this anisotropic structural change can be characterized as adaptation, resulting in emergent architectures and, ultimately, cell differentiation and secretion of extracellular matrix, *i.e.* appropriate tissue formation for predominant functional (mechanical) specifications.

A number of recent studies have underscored the interplay of cell and nucleus shape, mechanical properties, and remodeling during mechanotransduction and cell differentiation. However, cell shape [4,5,8], stiffness [9], and remodeling dynamics [10,11] are interrelated and the independent control of shape, stiffness, and/or remodeling to direct cellular differentiation still remains an intractable challenge. In a companion study (see Part A, preceding), we showed that prescribed seeding conditions as well as seeding density can be used to subject multipotent stem cells (MSCs) to volume changing stresses and that changes in volume of the cell are associated with changes in shape, but not volume, of the cell nucleus. In the current study, we aim to control the mechanical milieu of live cells while observing adapta-

tion of the cytoskeleton, a major cellular transducer that modulates cell shape, stiffness and remodeling. Taken in context of our working hypothesis, changes in the spatiotemporal organization of the cytoskeleton represent a structural adaptation to dynamic functional requirements. These functional requirements are defined by the developmental context of the stem cell, such as degree and duration of mechanical stress and surrounding cell density [3,12].

The cytoskeleton's ability to modulate the architecture and mechanical properties of the cell plays an essential role in cell differentiation [9,13,14]. Tubulin and actin are key cytoskeletal proteins involved in cell shape and mechanical properties, cellular signaling, metabolism, intracellular organization, transport, and biological responses to fluid flow [15,16]. Although high degrees of complexity exist in the interactions among cytoskeletal elements and their contributions to the mechanical properties of living cells, tubulin and actin are of particular interest since they exhibit vastly different mechanical properties as well as organization in determining cell architecture (Figure 1) [17]. Tubulin resists compression and contributes to cell viscosity. In contrast, actin resists tension, contributing to cell stiffness and resistance to deformation [18,19]. Hence, tubulin and actin elements of the cytoskeleton experience different mechanical stresses and consequently different temporal patterns of remodeling [20].

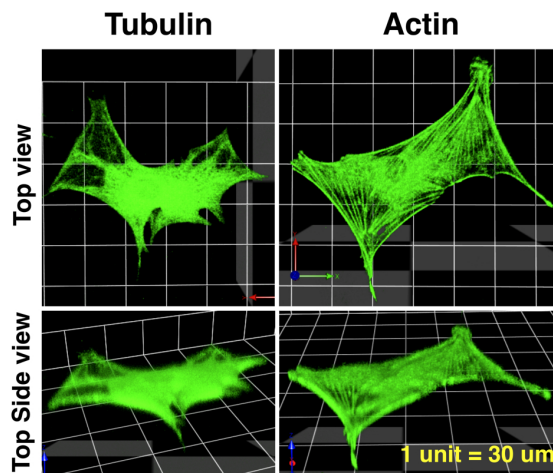


Figure 1: **Tubulin and actin cytoskeleton.** High resolution image stacks of the stem cell tubulin (left) and actin (right) cytoskeleton are acquired with a laser scanning confocal microscope and are reconstructed in three dimensions. These images are intentionally overexposed to clearly delineate the cytoskeletal boundaries.

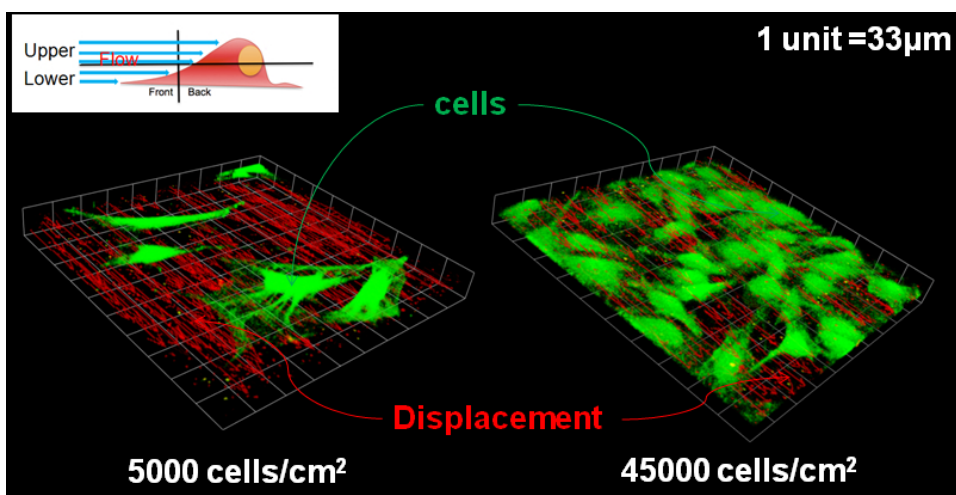


Figure 2: **3D images of flow fields around stem cells, reconstructed using micro-particle image velocimetry data and live cell imaging.** Red arrows indicate local flow velocity vectors, where microspheres displacements give vector magnitude and direction, around cells (green). The global flow direction is from the top left to the bottom right. Three dimensional confocal image stacks were analyzed to quantify the flow fields, spatiotemporally at subcellular scale resolution, with respect to distance from the substrate and cell density. After [23]. Used with permission.

The stem cell's mechanoadaptive response to deviatoric, shape changing stress (shear), and more specifically, the functional implications of cytoskeletal mechanoadaptation to shape changing stresses, are poorly understood, which provided the impetus for our recently published study where we mapped the live stem cell's mechanical milieu, spatially, temporally and at the subcellular scale [21] using computational fluid dynamics (CFD) predictions and micro particle image velocimetry ( $\mu\text{l-PIV}$ ). In addition, the approach provided a tool for real time observation and analysis of stem cell adaptation to the prevailing mechanical milieu, showing that the mechanical milieu of the stem cell exposed to fluid drag induced, shape changing shear stresses, varies with respect to proximity of surrounding cells as well as with respect to apical height (Figure 2) [21]. In addition to modulating fluid drag induced shear stresses by controlling precisely the direction and magnitude of the flow field to which the cells are exposed, shape changing deviatoric stresses are amplified in less densely seeded cells.

Hence, the goal of our current study is to elucidate adaptive changes in the cytoskeleton of MSCs in a controlled mechanical environment. We hypothesize that

the spatiotemporal organization of tubulin and actin elements of the cytoskeleton adapts in response to volume and shape changing stresses. Our approach was to measure components of the live MSC cytoskeleton in response to low magnitude, short duration, steady fluid flow induced shear stress (0.5 or 1.0 dyne/cm<sup>2</sup> for 30, 60, and 90 minutes), mimicking the mechanical stresses of embryonic stem cells prior to the first beating of the embryonic heart or the first twitch of skeletal muscle [3,4]. Previous studies showed that MSCs are much more sensitive to mechanical signals than mature, terminally differentiated cells [4,5,7]. The C3H/10T1/2 cells exhibit a similar degree of mechanosensitivity in genetic expression as stem cells, where their exposure to this magnitude and duration of mechanical stimulation results in a significant modulation of genes associated with the earliest markers of skeletogenesis, such as pre- (*Runx2* with *Msx2*) and peri-mesenchymal condensation (*Col1a1*, *Sox9*), as well as chondrogenesis (*Sox9* and *Col1a1*, and later *AGC* Aggrecan), osteogenesis (*Runx2* without *Msx2*), and adipogenesis (*Ppar-γ2*) [4,5]. Finally, taking into consideration the results of a recent study where we quantified the local mechanical milieu of cells seeded at similar densities and exposed to similar magnitude fluid drag induced shear stresses [21], we place the change in spatial distribution of tubulin and actin in context of the mechanical environment at the cellular scale.

## 2 Materials and Methods

### 2.1 Overview

Both the initial boundary conditions as well as the initial stress state of the MSC are prescribed through the cell density and seeding protocol. In a recent study we showed that seeding of cells at target densities, including defined “low” (LD, 5000 cells/cm<sup>2</sup>) and “high” densities (HD, 35,000 cells/cm<sup>2</sup>), exerts volume but not shape changing stresses on MSCs; with increasing density, cells decrease in volume and reach equilibrium after three days in culture [22]. In the current study, cells are imaged within 2 days in culture, and are thus in a state of compression at time zero, before application of shape changing shear stress by fluid flow. Cells seeded at LD are non-confluent and cells seeded at HD are confluent and in a single monolayer (Figure 3a) [4]. In a recently published study we showed that the mechanical environment of the MSC exposed to shape changing shear stresses induced by fluid flow varies with proximity of surrounding cells (density/confluency state) as well as with respect to distance from the substrate on which the cell is seeded [21].

To measure spatiotemporal changes in the cytoskeleton of in live MSCs, fluorescent actin and tubulin are measured at thirty-minute intervals in cells seeded at LD and HD and exposed to shape changing (shear) stresses [23] of 0.5 dynes/cm<sup>2</sup> and

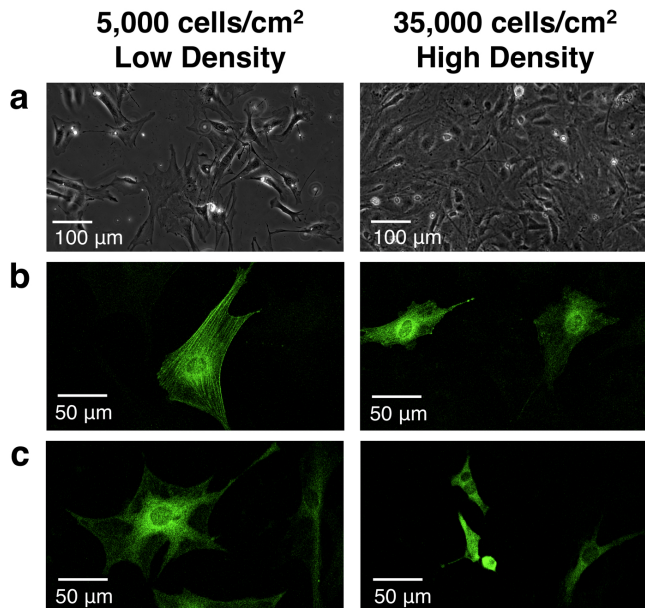


Figure 3: **Seeding density determines the initial mechanical stress state and boundary condition of the cells.** (a) Phase contrast image at 40x. Cells seeded at low density show little cell-cell contact and unoccupied substrate compared to those seeded at high density. Epifluorescent images at 100x of GFP-tagged (b) tubulin and (c) actin show that cells at low density exhibit larger cells with more defined cytoskeletal structures while cells at high density exhibit smaller cells with a less structured cytoskeleton. Note: Due to the less than 100% transfection efficiency of the fluorescent tag, we are able to identify individual cells, which would not be possible with perfect transduction or other labeling methods.

1 dyne/cm<sup>2</sup> via fluid flow for 90 minutes using a custom designed flow chamber designed to control the cellular environment, including gradients of biophysical and biochemical cues (in this study, a constant target shear stress was maintained without addition of exogenous biochemical cues) [1,2]. To assess cell shape changes due to flow, thickness of the tubulin and actin cytoskeleton is quantified as a function of cell density, shear stress magnitude, and time. To assess adaptation of MSCs to volume and shape changing stresses, intensity of tubulin and actin are quantified and normalized to the total volume of the cell. To quantify changes in tubulin and actin after exposure to shape changing stresses, we first measure changes in total concentration of tubulin and actin within each cell. We then measure the spatial

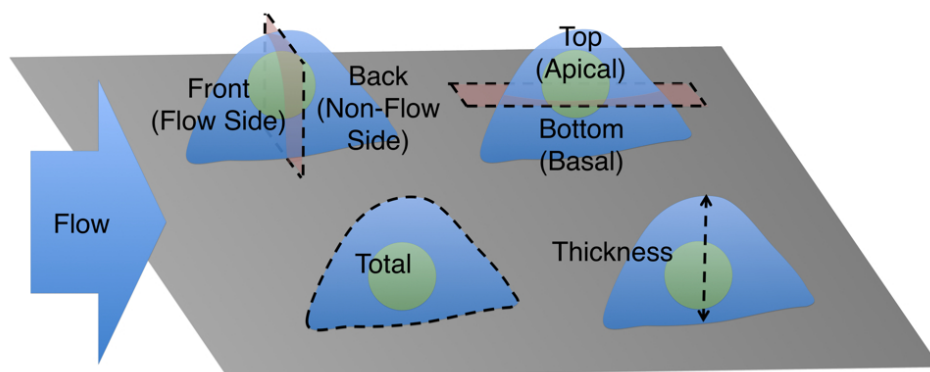


Figure 4: **Schematic diagram of reference points for cell measurements.** To measure mechanoadaptation quantitatively, normalized changes in intensities from a baseline control of fluorescent actin and tubulin are measured from the bisected regions along the direction of flow, in the front (flow-side) and back (non-flow-side) halves, and along the vertical profile of stem cells (apical-basal). The total amount of each fluorescent cytoskeletal element (tubulin, actin) as well its thickness is also measured.

distribution of actin and tubulin within each cell, normalized to the baseline control (not exposed to flow). Spatial distribution of the tubulin and actin cytoskeleton are measured with respect to relevant points of reference, from the cell's perspective, including the direction of flow (front – back) as well as the distance from the substrate on which the cell is seeded (defined by bisecting the cell in the apical-basal plane).

## 2.2 Cell Culture

Cells from a model MSC line [24] were used for the current study; the C3H/10T1/2 murine pluripotent embryonic cells are derived from the mesenchyme, do not show phenotypic drift, typical for primary cells derived from the mesoderm at E11.5 [3], and are capable of differentiating along several lineage paths, including osteogenic, chondrogenic, adipogenic, smooth muscle [8,25], and endothelial cell fates [4]. Cells were passaged in culture medium (Basal media eagle supplemented with 10% fetal bovine serum, 1% L-glutamine, and 1% penicillin/streptomycin [Invitrogen, Carlsbad, CA]) in T-75 culture flasks (Corning Inc., Corning, NY) and incubated at 37°C at 5% CO<sub>2</sub> in a humidified incubator until passage 3 (P3). At P3 cells were frozen and stored in cryovials at -80°C in culture medium with 40% fetal bovine serum and 10% DMSO. After storage, an additional passage was allowed for cell

proliferation such that all experiments were conducted on P5 cells. These cells were then detached using 0.25% trypsin-EDTA (Invitrogen, Carlsbad, CA) for 5 minutes, centrifuged, resuspended in fresh culture medium, and seeded on glass coverslips.

### **2.3 Coverslip Preparation**

One sterilized 25-mm plain glass coverslip (Fisher Scientific, Hampton, NH) was placed in each well of a six-well plate (Becton Dickinson, Franklin Lakes, NJ) and seeded with cells at specific densities in culture medium and incubated overnight to allow cells to adhere. Densities were measured using a hemocytometer.

### **2.4 Fluorescent tagging**

Cell tubulin and actin were fluorescently tagged one day after cell seeding using Cellular Lights<sup>TM</sup>actin-GFP and tubulin-GFP reagents (Invitrogen, Carlsbad, CA). These reagents target both polymerized as well as unpolymerized proteins. The protocol was slightly modified to account for the sensitivity of the cell line, where the transduction solution incubation time was reduced to 2 hours and the enhancing agent was used at 0.5 $\times$  and incubated overnight. Flow experiments were conducted the day after fluorescent tagging.

### **2.5 Shear Stress Magnitudes**

Fluid flow induced shear stress is applied at specific magnitudes and durations to mimic the effect of shape changing, deviatoric, stresses on the cytoskeleton of uncommitted MSCs. The custom-built parallel plate laminar flow chamber [1,2] was designed to impart highly controlled shear stresses of 0.5 or 1.0 dyne/cm<sup>2</sup> for 0 (immediately after application of shear stress), 30, 60, and 90 minutes.

### **2.6 Flow Experiments**

Prewarmed (37°C) culture media lacking fetal bovine serum was used as the flow medium because it was sterile, compatible with cells, and had a viscosity close to that of physiological saline. The flow medium was pumped through the flow chamber via a 60 ml syringe (Becton Dickinson, Franklin Lakes, NJ) placed in a screw pump (Harvard Apparatus, Holliston, MA). A non-flowed coverslip serves as a baseline control to account for the effects of flow as well as the possible effects of photobleaching over time. Cell densities and flow magnitudes were chosen to maximize control of the MSC stress state in order to elucidate mechanoadaptation in terms of structure-function relationships at the (sub)cellular length scale, and over a time scale relevant for events associated with mesenchymal condensation,

the initial stage of skeletogenesis that occurs over the course of up to 12 hours in the mesoderm of the mouse embryo, at 11.5 days gestation [3,21,22].

## 2.7 *Three Dimensional (3D) Imaging and Analysis*

Live cells were imaged in 3D prior to and during shear stress exposure, within the flow chamber, using a high-resolution laser scanning confocal microscope (SP2, Leica Microsystems, Mannheim, Germany). Fluorescent protein fluorescence was excited at 488 nm; separate cohorts of cells were used to study tubulin and actin adaptation, because fluorescent probes were only available in one excitation wavelength at the time of the experiment. Images were acquired at thirty minute intervals, using a 40 $\times$  objective (HCX APO L U-V-I 40.0 $\times$ 0.80 W), at a 498-555 nm emission wavelengths, with 1024 $\times$ 1024 pixel resolution and 0.2  $\mu$ m intervals between planar images with a numerical aperture of 0.8. Matlab (Mathworks, Natick, MA) was used to segment and to quantify fluorescence in the images.

The thickness of the fluorescence-tagged tubulin and actin was measured to assess shape changes due to deviatoric stress (flow induced shear). The intensity of the fluorescence was measured to assess concentration of tubulin and actin in space and time; similar to e.g. mineral density in the bony skeleton, intensity give a measure of "quality" if reported independent of spatial reference points [27]. Just as mineral distribution in space has significant consequences with regard to mechanical adaptation of a given bone to specifically oriented forces, the distribution of cytoskeletal tubulin and actin in space with respect to direction of flow and distance from the substrate and nearest neighbors [32] provides a measure of cellular mechanoadaptation. For this reason we measured intensities of the pixels (representing tubulin and actin distributions) in the total cell, as well as with respect to the front, back, apical, and basal regions of the cell (Figure 4). To keep regions consistent between cells within and between cohorts (experimental groups), reference points were always taken in a cellular context, similar to the definition of emergent polarity in the formation of epithelial sheets during development, where the apical and basal surfaces of the cell serve as reference points [28]. For example, flow direction is an absolute reference point defining the front and back of the cell with respect to the direction of shape changing forces to which the cell is subjected. Furthermore, the basal and apical edges of the cell are defined by the substrate on which the cell is seeded and the highest point of the cell from the substrate, respectively. The line of bisection between respective boundary edges (between front-back, apical-basal) defined regions with respect to cell-centric reference points.

Hence, by accounting for cell shape (thickness) as well as anisotropy (distribution of cytoskeletal elements in space), we can assess the adaptation of the cell to the shift in mechanical environment caused by volume and shape changing stresses.

To estimate changes attributable to volume changing stresses alone [22], we first compared total intensity of actin and tubulin in low density and high density cohorts (not exposed to flow). To account for changes attributable to shape changing stresses alone, we subtracted the intensities of baseline control (no flow) samples from those of samples exposed to flow. Reporting differences between flowed and unflowed samples also enabled us to negate photobleaching effects (since both cohorts were exposed to the laser for the same length of time). To account for natural variation in cell shape and size, intensity values were normalized to the values measured at time zero (just after the application of flow). Cells did not change in length over the 90 minute exposure to fluid flow.

Two dimensional (2D) image stacks were reconstructed into three dimensions (3D) using the image analysis software, Volocity (Improvision Inc., Waltham, MA). Transmitted and epifluorescent images were also taken at 40 $\times$  and 100 $\times$  magnification (LEICA DMIRE2; Leica Microsystems, Wetzlar, Germany) for qualitative assessment of cell shape and cytoskeletal structure.

## 2.8 Statistics

Statistical analysis of experimental data was performed using JMP (SAS, Cary, NC). Data for each variable group consisted of measurements from 9-10 cells, pooled from multiple experiments. Each experiment captured the data of 1-4 cells, where were processed and analyzed independently. Accounting for the sample size ( $n=9$ ) and lack of normal distribution, measurements were compared using a nonparametric two-sample Wilcoxon test. Significance was determined when  $\text{prob}>|z|$  was less than 0.05. Data from a previous study using identical cells, seeding densities, shear stress magnitude, and durations was used to compare cytoskeletal changes to changes in gene expression [4]. Nonparametric multivariate correlation analysis was performed using Spearman's  $\rho$ . Significance was determined when  $\text{prob}>|\rho|$  was less than 0.05.

## 3 Results

### 3.1 Overview: Effect of volume and shape changing stresses on cytoskeletal organization

Already before exposure to shape changing shear stresses, volume changing stresses imposed through seeding at target density markedly influence cytoskeletal organization. Qualitative observation of fluorescently tagged tubulin and actin in cells seeded at LD (5,000 cells/cm<sup>2</sup>) reveals larger appearing cells and more defined actin microfilaments and microtubules than cells seeded at HD (35,000 cells/cm<sup>2</sup>) (Figure 3b,c). Quantification of the total amount of tubulin and actin fluorescence

intensity within the cells, normalized to cell volume (measured in identical cohorts [22]) (Figure 5), show significantly lower total tubulin but no statistically significant differences in total actin in cells seeded at HD compared to LD.

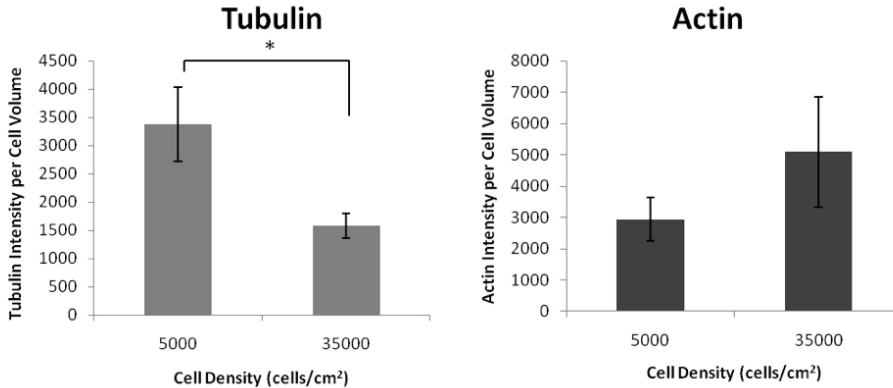


Figure 5: **Tubulin and actin concentration, normalized to cell volume, in LD and HD cells.** Normalized tubulin concentration is significantly higher in cells seeded at LD compared to HD and tends to be lower (albeit no statistical significance shown) in LD compared to HD cells. Asterisk (\*) indicates a significant difference ( $\text{prob} > |Z|$  was less than 0.05).

In general, the onset of fluid drag-induced shear stress (time zero measurements) is associated with an immediate change in vertical profile of the tubulin and actin cytoskeletons (*i.e.* the cytoskeletal thickness or apical-basal height, Figure 6a). This change depends significantly on the proximity to neighboring cells (density). Furthermore, the spatial distribution of cytoskeletal proteins changes as a function of location with respect to the direction of flow (Figure 6b) and distance from the substrate (Figure 6c) and duration of exposure to shape changing stresses. Due to the disparate structure-function relations and associated contrasting data trends inherent to the tubulin and actin cytoskeleton, we present detailed results in separate sections below.

### 3.2 Tubulin

#### Structure-Function Relationships

*Shape Changes:* Immediately with onset of flow, a striking and significant change in the vertical profile of the tubulin cytoskeleton is observed and is highly dependent on initial boundary conditions defined by cell density (distance to neighboring

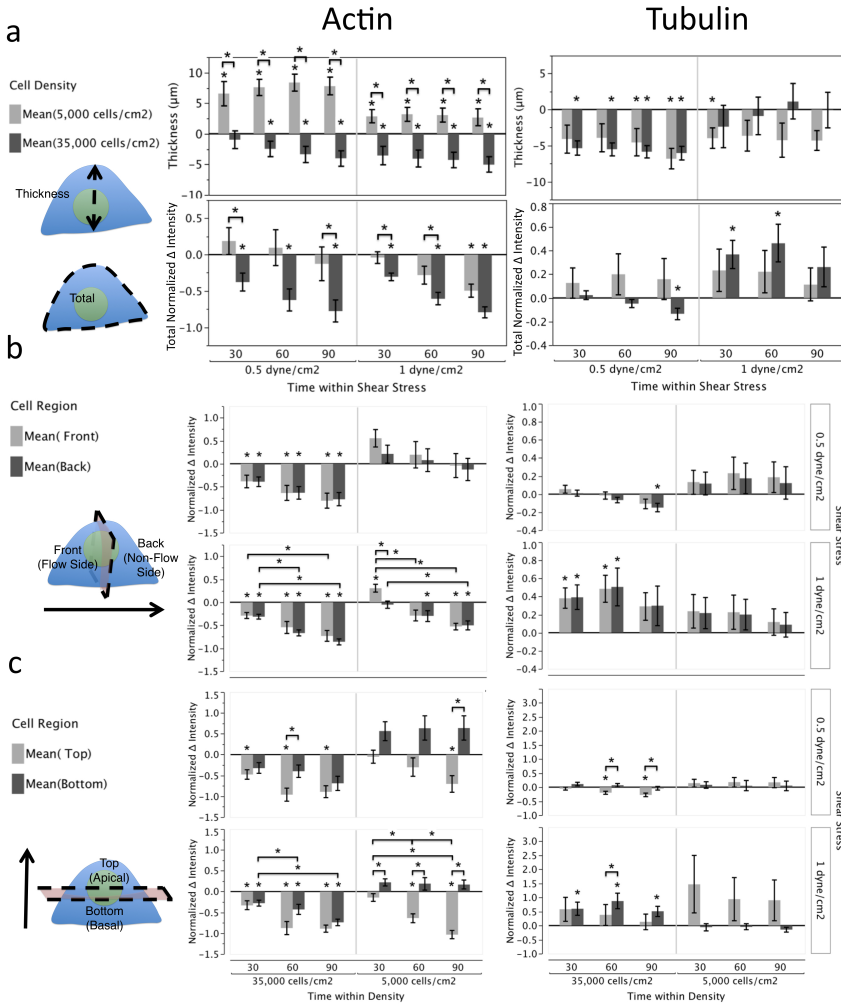


**Figure 6: Adaptation of tubulin and actin to shape changing stress exposure.** Changes from baseline of measured actin (right) and tubulin (left) over time at varying cell densities and shear stresses. (a) Changes in cell shape can be seen in the measurements of cytoskeletal thickness and total amount of cytoskeletal protein. (b) Emergent anisotropies in the direction of flow can be seen by comparing the front and back measurements of cytoskeletal protein. (c) Emergent anisotropies in the distance from the substrate can be seen by comparing the apical and basal measurements of cytoskeletal protein. Error bars show standard error; asterisks (\*) indicate a significant ( $\text{prob} > |Z|$  was less than 0.05) difference from zero and brackets indicate a significant ( $\text{prob} > |Z|$  was less than 0.05) differences in means.

cells, Figure 6a). Namely, in cells seeded at LD, the tubulin vertical profile significantly increases with onset of flow and, in cells seeded at HD, it significantly decreases with onset of flow. The increase in height of cells seeded at LD is smaller during exposure to  $1.0 \text{ dyn/cm}^2$  than  $0.5 \text{ dyn/cm}^2$  flow induced shear stress. The increase in height of cells seeded at LD and exposed to flow is not significantly different between time points, within or between cohorts subjected to either  $0.5$  or  $1.0 \text{ dyn/cm}^2$  shear stress. In the cells seeded at HD, the decrease in height of the tubulin cytoskeleton due to flow exposure does not change significantly between time points, within or between the cohorts subjected to either  $0.5$  or  $1.0 \text{ dyn/cm}^2$  shear stress. To put these data in context of initial height (prior to exposure to flow), data from a recent study measuring cell height using a cytoplasmic tag showed no significant difference in height of cells seeded at LD and HD [22].

*Concentration Changes:* With increasing time duration of exposure to shape changing stress, changes are more apparent in the concentration (as measured by fluorescence intensity) than in the thickness (height) of tubulin (Figure 6a). Whereas the concentration of tubulin increases initially with exposure to  $0.5 \text{ dyn/cm}^2$  shear stress, the concentration difference with respect to baseline decreases with time, resulting in an overall decrease from baseline after 90 minutes exposure to flow. In all other cohorts, including cells seeded at LD and exposed to  $1.0 \text{ dyn/cm}^2$  shear stress as well as both HD groups, tubulin concentration decreases immediately after exposure to shape changing stresses and tends toward a further decrease in tubulin concentration over time.

*Spatial Distribution: Emergent Anisotropy*

Exposure to shape changing stresses results in significant changes to the spatial distribution of tubulin concentration (as measured by change in intensity of fluorescence) that are highly dependent on proximity of other cells (density), distance from the substrate (apical-basal), and shear stress magnitude (Figure 6b,c). In general, cells seeded at LD shows greater anisotropy in distribution of tubulin concentration (greatest differences front-back and apical-basal), upon exposure to shape changing shear stress, than cells seeded at HD. Furthermore, emergence of anisotropy is more significantly influenced by effects of distance from the substrate than by the direction of flow.

The most striking pattern of emergent anisotropy is observed in cells seeded at LD and exposed to  $1.0 \text{ dyn/cm}^2$  shear stress, where exposure to flow results in an initial increase in tubulin concentration in the basal portion of the cell, persisting over time, and an initial decrease in tubulin concentration in the apical portion of the cell that decreases further (and significantly) with exposure time (Figure 6c); these changes in spatial distribution of tubulin are indicative of consistent mechanoadaptation at the (sub)cellular length scale. Furthermore, under these same density

and flow conditions, exposure to 30 minutes flow results in a significant increase in tubulin concentration in the front of the cell (flow side) but no significant change in the back of the cell. After 60 minutes, the tubulin concentration decreases below baseline in both the front and back of the cell, decreasing further at 90 minutes with no significant difference in concentration between the front and back of the cell.

In contrast, cells seeded at HD and exposed to both 0.5 and 1.0 dyn/cm<sup>2</sup> shear stress shows a significant decrease in tubulin concentration in both apical and basal regions of the cell (Figure 6c). Similar to cells seeded at LD, the basal tubulin concentration decreases significantly with time in cells seeded at HD, indicative of a consistent mechanoadaptation in the cytoskeleton to shear stress.

#### *Correlation with Gene Expression*

The increase in apical and non-flow side tubulin in a cell is negatively correlated with *Col1a1*, a marker of chondrogenesis. Furthermore, it is positively correlated with *Ppar-γ2*, a marker of adipogenesis. The non-flow side of tubulin is also positively correlated with *Sox9*, a marker of peri-mesenchymal condensation, and an earlier marker of chondrogenesis. The total amount of tubulin shows the same correlation with *Sox9* (Table 1). No correlation with *AGC* could be made, as exposure to flow completely abrogates aggrecan expression [4], a marker of chondrogenesis.

### **3.3 Actin**

#### *Structure-Function Relationships*

In general, shape and concentration changes over baseline in the actin cytoskeleton are more subtle than those observed in the tubulin cytoskeleton and cells seeded at HD show most significant mechanoadaptation in response to shear stress (Figure 6a). Cells seeded at HD exhibit a significant, rapid and persistent decrease in actin cytoskeleton thickness in response to 0.5 dyn/cm<sup>2</sup> shear stress exposure, with a significant decrease in actin concentration only after 90 minutes of exposure. In contrast, cells seeded at LD exhibit a significant decrease in height below baseline only after 60 minutes' exposure to flow, and this change in shape is not accompanied by a change in actin concentration. Interestingly, shape (thickness) and concentration trends are reversed with exposure to higher (1.0 dyn/cm<sup>2</sup>) shear stress. Only cells seeded at LD exhibit a significant decrease in actin cytoskeleton thickness, and only at the earliest observed time point. Whereas cells seeded at HD and exposed to 1.0 dyn/cm<sup>2</sup> shear stress exhibit no significant change in height of their actin cytoskeleton in response to flow, they do exhibit a significant increase in actin concentration at 30 and 60 minutes' flow exposure, with no significant difference from baseline 90 minutes after exposure to flow.

#### *Spatial Distribution: Emergent Anisotropy*

Flow induced changes in the spatial distribution of actin are also more subtle than those observed in the spatial distribution of tubulin (Figure 6b,c). Small but significant differences in actin distribution between the apical and basal regions of the cell are observed in cells seeded at HD after 60 minutes exposure to both 0.5 as well as 1.0 dyn/cm<sup>2</sup> flow (Figure 6c). This effect persists at 90 minutes exposure to the lower shear stress but becomes insignificant (statistically) in the higher stress group. No significant differences are observed in the distribution of actin between the front and back of the cell with respect to flow direction, for any of the groups studied (Figure 6b).

### C. Correlation with Gene Expression

The increase in actin in the flow, non-flow, apical, and basal sides of the cell, is negatively correlated with *Col3a1*, a marker of chondrogenesis. It is also negatively correlated with *Runx2*, a marker of pre-mesenchymal condensation as well as early chondrogenesis and osteogenesis. Furthermore, it is positively correlated with *Msx2*, a marker of pre-mesenchymal condensation (Table 1). As with tubulin, no correlation with *AGC* could be made, as exposure to flow completely abrogates aggrecan expression [4], a marker of chondrogenesis.

## 4 Discussion

Exposure of MSCs to minute volume and shape changing mechanical cues mimicking those that prevail *in utero* prior to the first heartbeat or twitch of skeletal muscle, results in significant changes to both tubulin and actin shape (height changes but not length), concentration (fluorescence intensity) and spatial distribution (anisotropic adaptation). Furthermore, the tubulin cytoskeleton adapts its mechanical structure with duration of exposure (time) to shape changing stresses induced by fluid flow. In addition, tubulin height and spatial distribution (concentration) exhibit striking differences attributable to the proximity of neighboring cells (density) as well as the substrate. Given a recently published study showing amplification of stress gradients (flow velocity) with increasing distance to nearest neighbors and the substrate, *i.e.* with decreasing density and toward the apical side of the cell, it appears that tubulin adaptation relates significantly to the magnitude of the stress to which the cell is exposed locally. Furthermore, contrasting responses are observed between flow magnitudes, implicating a "switch" in adaptive response. The actin cytoskeleton response to the changing mechanical milieu is more global, exhibiting less significant differences attributable to nearest neighbors or boundaries than differences attributable to magnitude of the stress to which the cell is exposed globally (0.5 versus 1.0 dyne/cm<sup>2</sup>). Recent data on strain stiffening behavior of actin networks may provide mechanistic insight into these observations [29]. Taken as a whole, exposure of MSCs to shape changing stresses, three orders of magnitude

**Table 1: Correlation of Cytoskeletal Changes to Gene Expression.** (top) Non-parametric Spearman's multivariate correlation analysis of cytoskeletal data and previously published data of mRNA changes from baseline of cells seeded at 35,000 cells/cm<sup>2</sup> exposed to 30 and 60 minutes of 1 dyne/cm<sup>2</sup> shear stress<sup>4</sup>. White (positive correlation) and black (negative correlation) elements indicate statistical significance in the correlation (Prob>| $\rho$ | less than 0.05). Grey elements indicate no statistically significant correlation. Aggrecan expression (AGC) was fully abrogated by exposure to shear stress and was hence not measurable (NM) or correlatable, in contrast to the previous study. (bottom) Reproduction of schematic depicting the timeline of condensation and fate commitment (yellow: pre-condensation, red dashed square: peri-condensation, orange: chondrogenesis, blue: osteogenesis, and green: adipogenesis), as a function of genetic markers (red text). In the mouse, mesenchymal condensation occurs at E11.5 or after 11.5 days gestation. *After* [3]. Used with permission.

P-values		Relative Fold Change in Gene Expression						
		Msx2	Col1A	Runx2	Sox9	Col2A	AGC	PparG
Cytoskeletal protein measurements	<b>Tubulin</b> thickness	0.1437	0.6666	0.1981	0.9926	0.1380	NM	0.7434
	<b>Tubulin</b> total	0.0387	0.5604	0.6326	0.0239	0.0983	NM	0.4336
	<b>Tubulin</b> flow side	0.9330	0.8665	0.9926	0.1195	0.0878	NM	0.2477
	<b>Tubulin</b> non-flow side	0.5477	0.3235	0.6126	0.0172	0.0015	NM	0.0042
	<b>Tubulin</b> apical	0.6461	0.2774	0.6529	0.1005	0.0016	NM	0.0022
	<b>Tubulin</b> basal	0.5733	0.8008	0.6529	0.2239	0.6598	NM	0.7012
	<b>Actin</b> thickness	0.1495	0.9330	0.2999	0.5994	0.4623	NM	0.1647
	<b>Actin</b> total	0.3381	0.6126	0.1145	0.4336	0.3480	NM	0.9034
	<b>Actin</b> flow side	0.0104	0.1195	0.0155	0.2908	0.0255	NM	0.5351
	<b>Actin</b> non-flow side	0.0410	0.0627	0.0387	0.5863	0.0178	NM	0.3737
	<b>Actin</b> apical	0.0325	0.0878	0.0398	0.5351	0.0150	NM	0.3235
<b>Actin</b> basal	0.0247	0.0659	0.0204	0.3633	0.0458	NM	0.5103	

smaller than those prevailing in the mature skeleton during physiological activity but of a time and length scale consistent with mechanical cues prevailing *in utero* during mesenchymal condensation, results in emergent anisotropy of cytoskeletal architecture.

The adaptation of the tubulin and actin cytoskeleton to shape changing stress reflects both the mechanical function of these cytoskeletal proteins as well as the balance of forces at cell boundaries. At initial exposure to flow, cells seeded at LD and HD have very different boundary conditions. Although cells seeded at LD and HD show similar height, cells seeded at LD are isolated from their neighbors albeit in maximal contact with the flow field. In contrast, cells seeded at HD are in

a confluent monolayer, surrounded by neighboring cells except on apical surfaces that are in contact with the flow field. Furthermore, in contrast to the tubulin cytoskeleton which acts as a damper, resisting forces that compress the cell, the actin cytoskeleton acts like an elastic rope or spring to resist forces pulling on the cell [19]. Isolated cells (seeded at LD) are exposed to highest shape changing forces with intrinsic compressive components [21], pushing the cell up from the side and resulting in an increase in tubulin concentration that is highest on apical surfaces of cells that are exposed to highest stresses and that decreases significantly over time as the cell adapts. In contrast, cells seeded at HD abut one another; with exposure to flow, the monolayer deforms as a whole, with its tubulin cytoskeleton decreasing in height and concentration over time, indicative of mechanoadaptation.

In contrast, the actin cytoskeleton exhibits disparate adaptation dependent on shear stress magnitude, with fewer differences attributable to boundary conditions (seeding density), direction of flow, or distance from the substrate on which cells are seeded. Cells seeded at HD exhibit a significant, rapid and persistent decrease in actin cytoskeleton thickness in response to  $0.5 \text{ dyn/cm}^2$  shear stress exposure, with a significant decrease in actin concentration only after 90 minutes of exposure; this may provide insight into mechanisms of adaptation where immediate (passive) adaptation due to changes in force balance at the cell boundary, manifested through changes in cell shape (height), result in downstream decrease in concentration of actin (active). Furthermore, the lack of emergent anisotropy in response to shape changing shear stress exposure may reflect the combined pushing and pulling of actin cytoskeletal elements resulting from lateral, unidirectional compression of individual cells as well as vertical compression of confluent cell layers. Interestingly, the actin cytoskeleton exhibits markedly disparate behavior in response to the  $0.5$  and  $1.0 \text{ dyn/cm}^2$  shear magnitudes, potentially indicative of strain stiffening behavior [29]. Namely, finite element simulations were used recently to study the elastic response of actin networks with compliant and rigid cross links. Accounting for different stiffnesses of cross linkers, it could be shown that the deformation of networks with compliant cross linkers results in strain stiffening behavior not observed in networks cross linked with rigid cross linkers. This is due to the fact that, compliant cross linkers first extend fully, resulting in deformation of the network filaments; with increasing applied strain, the filaments deform further, resulting in a stiffened elastic response.

The correlation data, on the other hand, reveal some interesting association between cytoskeletal arrangement and gene expression. While this data suggests correlation rather than causation, it is still able to tie structural adaptation of the cell to genetic adaptation in response to shear stress. These results seem to suggest an important link between tubulin architecture, chondrogenesis, and adipogenesis. There is also

an important link between actin architecture and pre-mesenchymal condensation. Our data is not able to determine if tubulin or actin architecture triggers changes in gene expression, gene expression triggers changes in cytoskeletal organization, or if a more complex relationship exists. Although actin and tubulin have many different roles in all types of cells and functions, these new findings highlight the importance of cytoskeletal organization and distribution in stem cell fate.

Accounting for the functional roles of tubulin and actin, respectively, one might envision the cell as a tent in which tubulin elements act like the pre-tensioned poles that prevent collapse of the tent and actin elements are analogous to the elastic reinforcements in the fabric that keep the tent from being pulled away by wind and weather; integrins (or other non-junctional adhesions) or focal adhesions (or other junctional adhesions) that anchor the cytoskeleton to the matrix or substrate would be analogous to the stakes that keep the tent securely fastened to the ground. By setting up multiple tents in close proximity, downwind tents are sheltered. Previous computational models from our group as well as recent experimental studies of fluid flow around MSCs (Figure 1) predict and demonstrate, respectively, that for a given global flow field, isolated cells experience higher stress magnitudes than confluent cells [3,21]. Furthermore, for isolated cells, the cell is subjected to shear stress via fluid drag, from basal to apical surfaces, with magnitude increasing toward the apical edges of the cell [19]. In contrast, confluent cells experience little stress near basal surfaces and the majority of the shear stress on their apical surfaces. Hence, although cohorts of cells seeded at LD and HD, respectively, are subjected to identical global flow fields (0.5 and 1.0 dyn/cm<sup>2</sup>, applied in a controlled fashion using a custom designed flow chamber [26]), their local mechanical milieu are inherently disparate at the length scale of the cell. In fact, the mechanical milieu of cells seeded at LD and HD are distinct at the subcellular scale, showing directional differences with regard to cell-centric reference points including the leading and trailing edge of the cell (defined by flow direction) as well as the apical and basal surface of the cell. We are currently developing methods to map cell strains and cytoskeletal remodeling concomitant to mapping of flow fields around cells, which should yield further key information regarding potential effects of flow field nonuniformities, including shear gradients, different temporal patterns of flow including pulsatile flow, and different stiffnesses of undifferentiated and differentiated cells [35].

Our results confirm that cytoskeletal remodeling patterns in pluripotent cells are markedly different from those reported in more mature, differentiated cells. Whereas mature endothelial cells required a much larger shear stress, from 15 to 20 dynes/cm<sup>2</sup>, applied for a much longer duration of 12-24 hours to effect changes in baseline reflective of mechanoadaptation [25], undifferentiated pluripotent cells show changes

in baseline behavior in response to much smaller magnitude shear stresses. This discrepancy may reflect not only the higher mechanosensitivity of MSCs observed previously [4] but also the physiological context of the mechanical environment to which these cells are usually subjected. Furthermore, endothelial cells possess specialized intracellular and extracellular mechanosensors and mechanotransducers that play a critical role in their adaptive patterns [30, 31]. Endothelial cells also change alignment in response to flow direction [32,33].

Similar to other published studies [8], several limitations to the current study design are inherent to our means of controlling cell boundaries and force balances at cell boundaries. For instance, the current study does not account for cell-cell interactions. While the low density seeding protocols still permit some cell-cell contact, intercellular communication is not controlled or considered in this study. Furthermore, at the time the study was carried out, no fluorescent tagging agents were available to distinguish between unpolymerized and polymerized cytoskeletal proteins; follow on studies implement the newest tagging agents that will allow for unprecedented tracking of emergent anisotropy in the architecture of the cytoskeleton. In addition to our inability to assess whether adaptation is active or passive in the current study, the size of the data sets generated and the imperative to minimize effects of photobleaching limited the time resolution of our study to 30 minute intervals. The resulting time scale and resolution may not have been sufficient to capture every possible pattern of cytoskeletal remodeling. Further study, examining smaller regions of the cell or tracking changes in individual filaments or orientation in real time, could provide further insight.

In conclusion, we present a novel spatiotemporal analysis of a model stem cell cytoskeletal mechanoadaptation that reveals a more organized and directed response to shear stress than previously known. The current study emphasizes the importance of mechanical signals and a cellular context for understanding development, growth, adaptation, healing, and engineering of tissues by their cellular constituents. Given the currently observed mechanical adaptation of stem cells to their dynamic local milieu, in light of previous studies demonstrating the effect of cells themselves on local flow fields [21], it appears that stem cells may ultimately exhibit the capacity to modulate their own environment by altering their structure. At the length scale of the cell, such mechanoadaptation redistributes forces at interfaces between the cell and its environment. At higher length scales, cells within multicellular structures modulate force balances at boundaries not only through adaptation of their own architecture but also through specialization of higher order structure, enabling function in the prevailing mechanical environment. Taken as a whole, these studies support our overarching hypothesis that, already at earliest stages of life, mechanical function inherent to life on Earth modulates the emer-

gence of cellular architecture and multicellular structure [3,35]. Finally, quantification of the spatiotemporal patterns of stem cell remodeling in response to easily controllable variables such as cell density and applied external forces may provide a platform for engineers and scientists to direct short-term structure function relationships and long-term fate decisions. The field of cytoskeletal epigenetics is evolving rapidly, as the structure of cells are shown to play a much larger role in cell memory and cell fate than previously assumed [35,36].

**Acknowledgement:** We thank Brian Wodlinger for assistance with Matlab and Joshua Zimmermann for assistance with cell culture and cell volume analysis. This study was supported by the National Science Foundation, Grant #CMMI-0826435 (Nano Bio Mechanics Program). Hana Chang was supported through a Medtronic Fellowship, the NSF Grant, and a National Institutes of Health Musculoskeletal T32 Training Grant (NIH/ NIAMS 2T32AR007505).

## References

1. Anderson, E.J., Falls, T.D., Sorkin, A.M., & Knothe Tate, M.L. (2006) *Biomed Eng Online*. 5, 27.
2. Anderson, E.J., & Knothe Tate, M.L. (2007) *Biomed Eng Online*. 6, 46.
3. Knothe Tate, M.L., Falls, T.D., McBride, S.H., Atit, R., & Knothe, U.R. (2008) *Int. J. Biochem. Cell Biol.* 40, 2720–2738.
4. McBride, S.H., Falls, T., & Knothe Tate, M.L. (2008) *Tissue Eng.*, Part A 14, 1573-1580.
5. McBride, S.H. & Knothe Tate, M.L. (2008) *Tissue Eng.*, Part A 14, 1561-1572.
6. Engler, A.J., Sen, S., Sweeney, H.L., & Discher, D.E. (2006) *Cell* 126, 677–689.
7. Oberhofer, K. (2005) Diploma Thesis, Swiss Federal Institute of Technology, Zurich.
8. McBeath, R., Pirone, D.M., Nelson, C.M., Bhadriraju, K., & Chen, C.S. (2004) *Dev. Cell* 6, 483-495.
9. Titushkin, I. & Cho, M. (2007) *Biophys. J.* 93, 3693-3702.
10. Janmey, P.A. & McCulloch, C.A. (2007) *Annu. Rev. Biomed. Eng.* 9, 1-34.

11. Wang, N. & Ingber, D.E. (1994) *Biophys. J.* 66, 2181-2189.
12. Sims, J.R., Karp, S., Ingber, D.E. (1992) *J. Cell. Sci.* 103, 1215-1222.
13. Clowes-Arnsdorf, E.J., Kwon, R.Y., Tummala, P., Carter, D.R., & Jacobs, C.R. (2006) *MCB: Mol. Cell. Biomech.* 3, 205-206.
14. Yourek, G., Hussain, M.A., & Mao, J.J. (2007) *Am. Soc. Artif. Intern. Organs J.* 53, 219-228.
15. Chen, N.X., Ryder, K.D., Pavalko, F.M., Turner, C.H., Burr, D.B., Qiu, J., & Duncan, R.L. (2000) *Am. J. Physiol. Cell Physiol.* 278, C989-997.
16. Cooper, J.A. (1987) *J. Cell Biol.* 105, 1473-1478.
17. Fletcher, D.A. & Mullins, R.D. (2010) *Nature* 463, 485-492.
18. Wang, N. (1998) *Hypertension* 32, 162-165.
19. Wang, N., Naruse, K., Stamenovic, D., Fredberg, J.J., Mijailovich, S.M., Tolic-Nørrelykke, I.M., Polte, T., Mannix, R., & Ingber, D.E. (2001) *Proc. Natl. Acad. Sci. USA* 98, 7765-7770.
20. Gardel, M., Kasza, K., Brangwynne, C., Liu, J., & Weitz, D. (2008) *Methods Cell Biol.* 89, 487-519.
21. Song, M.J., Dean, D., & Knothe Tate, M.L. (2010) *PLoS One* 5, e12796.
22. Zimmermann, J. & Knothe Tate, M.L. (2011) *MCB: Mol Cell Biotech* 187.
23. Alenghat, F.J. & Ingber, D.E. (2002) *Sci. STKE* 2002, pe6.
24. Guilak, F., Cohen, D.M., Estes, B.T., Gimble, J.M., Liedtke, W., & Chen C.S. (2009) *Cell Stem Cell* 5, 17-26.
25. Malek, A. & Izumo, S. (1996) *J. Cell Sci.* 109, 713-726.
26. Knothe, U.R., Dolejs, S., Miller, R.M., & Knothe Tate, M.L. (2010) *J. Biomech.* 43, 2728-2737.
27. Morali, O., Savagner, P., & Larue, L. (2005) *Madame Curie Bioscience Database* (Landes Bioscience, Austin, TX), pp. 12-5.
28. Chen, P. & Shenoy, V.B. (2011) *Soft Matter* 7, 355-358.
29. Park, B., Hah, Y., Kim, D., Kim, J., & Byun, J. (2008) *Oral Surg. Oral Med. Oral Pathol. Oral Radiol. Endod.* 105, 554-560.

30. Chien, S. (2007) *Am. J. Physiol. Heart Circ. Physiol.* 292, H1209-24.
31. Wechezak, A.R., Wight, T.N., Viggers, R.F. & Sauvage, L.V. (1985) *Lab Invest* 53, 639-647.
32. Kim, D.W., Gottlieb, A.I. & Langille, B.L. (1989) *Arteriosclerosis* 9, 439-445.
33. Knothe Tate, M.L. & Falls, T. (2010) *Fields Communications* 57, 1-22.
34. Locke, M. (1990) *J. Cell Sci.* 96, 563–567.
35. Sato, M., Levesque, M.J., & Nerem, R.M. (1987) *Arteriosclerosis* 7, 276–286.
36. Pillarisetti A, Desai JP, Ladjal H, Schiffmacher A, Ferreira A, Keefer CL. (2011) *Cell Reprogram* 13, 371-80.